

Weak Decays of B_s Mesons

R.N. Faustov¹, V.O. Galkin¹

¹Dorodnicyn Computing Centre, Russian Academy of Sciences, Vavilov Str. 40, 119333 Moscow, Russia

The branching fractions of the semileptonic and rare B_s decays are calculated in the framework of the QCD-motivated relativistic quark model. The form factors of the weak B_s transitions are expressed through the overlap integrals of the initial and final meson wave functions in the whole accessible kinematical range. The momentum transfer dependence of the form factors is explicitly determined without additional model assumptions and extrapolations. The obtained results agree well with available experimental data.

1 Introduction

In recent years significant experimental progress has been achieved in studying properties of B_s mesons. The Belle Collaboration considerably increased the number of observed B_s mesons and their decays due to the data collected in e^+e^- collisions at the $\Upsilon(10860)$ resonance [1]. On the other hand, B_s mesons are copiously produced at Large Hadron Collider (LHC). First precise data on their properties are coming from the LHCb Collaboration. Several weak decay modes of the B_s meson were observed for the first time [2]. New data are expected in near future.

In this lecture we consider the weak B_s transition form factors and decay rates in the framework of the relativistic quark model based on the quasipotential approach in quantum chromodynamics (QCD) [4]. We previously applied this model for the calculation of the weak B transitions [5]. Recently Belle and BaBar Collaborations [3] published new more precise data on differential distributions in $B \rightarrow \pi l \nu_l$ and $B \rightarrow \rho l \nu_l$ decays. In Fig. 1 we compare predictions of our model with these data. From this figure we see that our predictions agree well with new data. The fit of our model predictions to the combined Belle and BaBar data yields the following values of the CKM matrix element V_{ub}

- $B \rightarrow \pi l \nu_l$ decays $|V_{ub}| = (4.07 \pm 0.07_{\text{exp}} \pm 0.21_{\text{theor}}) \times 10^{-3}$
- $B \rightarrow \rho l \nu_l$ decays $|V_{ub}| = (4.03 \pm 0.15_{\text{exp}} \pm 0.21_{\text{theor}}) \times 10^{-3}$
- combined data on $B \rightarrow \pi(\rho) l \nu_l$ $|V_{ub}| = (4.06 \pm 0.06_{\text{exp}} \pm 0.21_{\text{theor}}) \times 10^{-3}$

These values are in good agreement with the averaged value extracted from the inclusive B decays [6] $|V_{ub}| = (4.41 \pm 0.15^{+0.15}_{-0.19}) \times 10^{-3}$.

2 Relativistic quark model

All considerations in this lecture are done in the framework of the relativistic quark model. The model is based on the quasipotential approach in quantum field theory with the QCD motivated

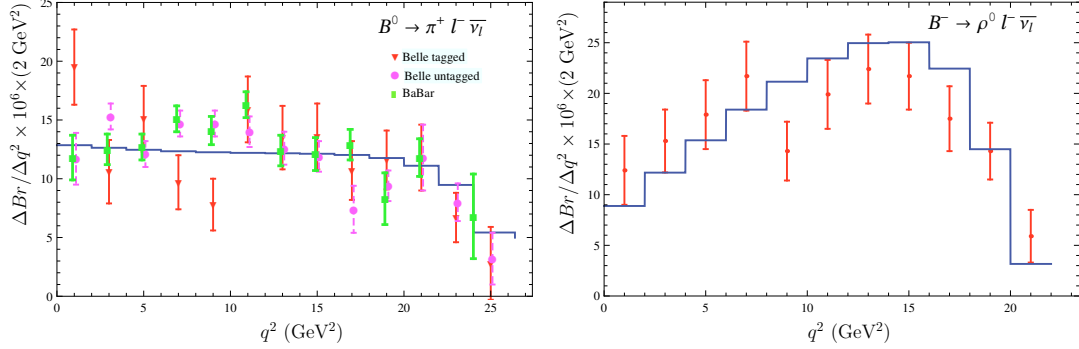


Figure 1: Comparison of predictions of our model with the recent experimental data (Belle 2011, 2013; BaBar 2012) for the $B^0 \rightarrow \pi^+ l^- \bar{\nu}_l$ decay and Belle (2013) data for the $B \rightarrow \rho l \nu$ decay.

interaction. Hadrons are considered as the bound states of constituent quarks and are described by the single-time wave functions satisfying the three-dimensional Schrödinger-like equation, which is relativistically invariant [7]:

$$\left(\frac{b^2(M)}{2\mu_R} - \frac{\mathbf{p}^2}{2\mu_R} \right) \Psi_M(\mathbf{p}) = \int \frac{d^3q}{(2\pi)^3} V(\mathbf{p}, \mathbf{q}; M) \Psi_M(\mathbf{q}), \quad (1)$$

where

$$\mu_R = \frac{M^4 - (m_1^2 - m_2^2)^2}{4M^3}, \quad b^2(M) = \frac{[M^2 - (m_1 + m_2)^2][M^2 - (m_1 - m_2)^2]}{4M^2}, \quad (2)$$

M is the meson mass, $m_{1,2}$ are the quark masses, and \mathbf{p} is their relative momentum. The interaction quasipotential $V(\mathbf{p}, \mathbf{q}; M)$ consists of the perturbative one-gluon exchange part and the nonperturbative confining part [7]. The Lorentz structure of the latter part includes the scalar and vector linearly rising interactions. The long-range vector vertex contains the Pauli term (anomalous chromomagnetic quark moment) which enables vanishing of the spin-dependent chromomagnetic interaction in accord with the flux tube model.

For the consideration of the meson weak decays it is necessary to calculate the matrix element of the weak current between meson states. In the quasipotential approach, such a matrix element between a B_s meson with mass M_{B_s} and momentum p_{B_s} and a final F meson with mass M_F and momentum p_F is given by [7]

$$\langle F(p_F) | J_\mu^W | B_s(p_{B_s}) \rangle = \int \frac{d^3p d^3q}{(2\pi)^6} \bar{\Psi}_{F \mathbf{p}_F}(\mathbf{p}) \Gamma_\mu(\mathbf{p}, \mathbf{q}) \Psi_{B_s \mathbf{p}_{B_s}}(\mathbf{q}), \quad (3)$$

where $\Gamma_\mu(\mathbf{p}, \mathbf{q})$ is the two-particle vertex function and $\Psi_{M \mathbf{p}_M}(\mathbf{p})$ are the meson ($M = B_s, F$) wave functions projected onto the positive energy states of quarks and boosted to the moving reference frame with momentum \mathbf{p}_M , and \mathbf{p}, \mathbf{q} are relative quark momenta.

The explicit expression for the vertex function $\Gamma_\mu(\mathbf{p}, \mathbf{q})$ can be found in Ref. [4]. It contains contributions both from the leading order spectator diagram and from subleading order diagrams accounting for the contributions of the negative-energy intermediate states. The leading

order contribution contains the δ function which allows us to take one of the integrals in the matrix element (3). Calculation of the subleading order contribution is more complicated due to the dependence on the relative momentum in the energies of the initial heavy and final light quarks. For the energy of the heavy quarks we use heavy quark expansion. For the light quark such expansion is not applicable. However, if the final F meson is light (K, φ etc.) than it has a large (compared to its mass) recoil momentum ($|\mathbf{\Delta}_{\max}| = (M_{B_s}^2 - M_F^2)/(2M_{B_s}) \sim 2.6$ GeV) in almost the whole kinematical range except the small region near $q^2 = q_{\max}^2$ ($|\mathbf{\Delta}| = 0$). This also means that the recoil momentum of the final meson is large with respect to the mean relative quark momentum $|\mathbf{p}|$ in the meson (~ 0.5 GeV). Thus one can neglect $|\mathbf{p}|$ compared to $|\mathbf{\Delta}|$ in the light quark energies $\epsilon_q(p + \Delta) \equiv \sqrt{m_q^2 + (\mathbf{p} + \mathbf{\Delta})^2}$, replacing it with $\epsilon_q(\Delta) \equiv \sqrt{m_q^2 + \mathbf{\Delta}^2}$ in expressions for the subleading contribution. Such replacement removes the relative momentum dependence in the energies of quarks and thus permits the performance of one of the integrations in the subleading contribution using the quasipotential equation. Since the subleading contributions are suppressed the uncertainty introduced by such procedure is small. As a result, the weak decay matrix element is expressed through the usual overlap integral of initial and final meson wave functions and its momentum dependence can be determined in the whole accessible kinematical range without additional assumptions.

3 Semileptonic B_s decays to D_s mesons

The matrix elements of weak current J^W between meson ground states are usually parametrized by the following set of the invariant form factors

$$\langle D_s(p_{D_s}) | \bar{c} \gamma^\mu b | B_s(p_{B_s}) \rangle = f_+(q^2) \left[p_{B_s}^\mu + p_{D_s}^\mu - \frac{M_{B_s}^2 - M_{D_s}^2}{q^2} q^\mu \right] + f_0(q^2) \frac{M_{B_s}^2 - M_{D_s}^2}{q^2} q^\mu, \quad (4)$$

$$\langle D_s^*(p_{D_s^*}) | \bar{c} \gamma^\mu b | B(p_{B_s}) \rangle = \frac{2iV(q^2)}{M_{B_s} + M_{D_s^*}} \epsilon^{\mu\nu\rho\sigma} \epsilon_\nu^* p_{B_s\rho} p_{D_s^*\sigma}, \quad (5)$$

$$\begin{aligned} \langle D_s^*(p_{D_s^*}) | \bar{c} \gamma^\mu \gamma_5 b | B_s(p_{B_s}) \rangle &= 2M_{D_s^*} A_0(q^2) \frac{\epsilon^* \cdot q}{q^2} q^\mu + (M_{B_s} + M_{D_s^*}) A_1(q^2) \left(\epsilon^{*\mu} - \frac{\epsilon^* \cdot q}{q^2} q^\mu \right) \\ &\quad - A_2(q^2) \frac{\epsilon^* \cdot q}{M_{B_s} + M_{D_s^*}} \left[p_{B_s}^\mu + p_{D_s^*}^\mu - \frac{M_{B_s}^2 - M_{D_s^*}^2}{q^2} q^\mu \right]. \end{aligned} \quad (6)$$

To calculate the weak decay matrix element we employ the heavy quark expansion, which permits us to take one of the integrals in the subleading contribution of the vertex function to the weak current matrix element. As a result we express all matrix elements through the usual overlap integrals of the meson wave functions. We find that the decay form factors can be approximated with sufficient accuracy by the following expressions:

$$(a) \quad f_+(q^2), V(q^2), A_0(q^2) = F(q^2) = \frac{F(0)}{\left(1 - \frac{q^2}{M^2}\right) \left(1 - \sigma_1 \frac{q^2}{M_{B_c^*}^2} + \sigma_2 \frac{q^4}{M_{B_c^*}^4}\right)}, \quad (7)$$

$$(b) \quad f_0(q^2), A_1(q^2), A_2(q^2) = F(q^2) = \frac{F(0)}{\left(1 - \sigma_1 \frac{q^2}{M_{B_c^*}^2} + \sigma_2 \frac{q^4}{M_{B_c^*}^4}\right)}, \quad (8)$$

where $M = M_{B_c^*} = 6.332$ GeV for the form factors $f_+(q^2)$, $V(q^2)$ and $M = M_{B_c} = 6.272$ GeV for the form factor $A_0(q^2)$; the values $F(0)$ and $\sigma_{1,2}$ are given in Table 1. The values of $\sigma_{1,2}$ are determined with a few tenths of percent errors. The main uncertainties of the form factors originate from the account of $1/m_Q^2$ corrections at zero recoil only and from the higher order $1/m_Q^3$ contributions and can be roughly estimated in our approach to be about 2%.

	$B_s \rightarrow D_s$		$B_s \rightarrow D_s^*$			
	f_+	f_0	V	A_0	A_1	A_2
$F(0)$	0.74	0.74	0.95	0.67	0.70	0.75
$F(q_{\max}^2)$	1.15	0.88	1.50	1.06	0.84	1.04
σ_1	0.200	0.430	0.372	0.350	0.463	1.04
σ_2	-0.461	-0.464	-0.561	-0.600	-0.510	-0.070

Table 1: Form factors of weak $B_s \rightarrow D_s^{(*)}$ transitions.

In Table 2 we confront our predictions for the form factors of semileptonic decays $B_s \rightarrow D_s^{(*)} e \nu$ at maximum recoil point $q^2 = 0$ with results of other approaches [8, 9, 10, 11, 12]. Different quark models are used in Refs. [8, 10, 12], while the QCD and light cone sum rules are employed in Refs. [9, 11]. We find that these significantly different theoretical calculations lead to rather

	$f_+(0)$	$V(0)$	$A_0(0)$	$A_1(0)$	$A_2(0)$
our	0.74 ± 0.02	0.95 ± 0.02	0.67 ± 0.01	0.70 ± 0.01	0.75 ± 0.02
[8]	0.61	0.64		0.56	0.59
[9]	0.7 ± 0.1	0.63 ± 0.05	0.52 ± 0.06	0.62 ± 0.01	0.75 ± 0.07
[10]	$0.57^{+0.02}_{-0.03}$	$0.70^{+0.05}_{-0.04}$		$0.65^{+0.01}_{-0.01}$	$0.67^{+0.01}_{-0.01}$
[11]	$0.86^{+0.17}_{-0.15}$				
[12]		$0.74^{+0.05}_{-0.05}$	$0.63^{+0.04}_{-0.04}$	$0.61^{+0.04}_{-0.04}$	$0.59^{+0.04}_{-0.04}$

Table 2: Comparison of theoretical predictions for the form factors of semileptonic decays $B_s \rightarrow D_s^{(*)} e \nu$ at maximum recoil point $q^2 = 0$.

close values of the decay form factors. One of the main advantages of our model is its ability not only to obtain the decay form factors at the single kinematical point, but also to determine its q^2 dependence in the whole range without any additional assumptions or extrapolations.

Using these weak decay form factors we calculate the total semileptonic decay rates. It is necessary to point out that the kinematical range accessible in these semileptonic decays is rather broad. Therefore the knowledge of the q^2 dependence of the form factors is very important for reducing theoretical uncertainties of the decay rates. Our results for the semileptonic $B_s \rightarrow D_s^{(*)} l \nu$ decay rates are given in Table 3 in comparison with previous calculations. The authors of Ref.[9] use the QCD sum rules, while the light cone sum rules approach is adopted in Ref. [11]. Different types of constituent quark models are employed in Refs. [12, 10, 13] and the three point QCD sum rules are used in Ref. [14]. We see that our predictions are consistent with results of quark model calculations in Refs. [12, 10]. They are approximately two times larger than the QCD sum rules and light cone sum rules results of Refs. [9, 11], but slightly lower than the values of Refs. [13, 14].

Using the same approach we calculate the form factors of B_s decays to radially and orbitally excited D_s mesons. The predictions for the branching fractions for B_s decays to radially excited D_s mesons are given in Table 4. We find that semileptonic B_s decays to the pseudoscalar

Decay	this paper	[9]	[10]	[11]	[12]	[13]	[14]
$B_s \rightarrow D_s e \nu$	2.1 ± 0.2	1.35 ± 0.21	1.4-1.7	$1.0^{+0.4}_{-0.3}$		2.73-3.00	2.8-3.8
$B_s \rightarrow D_s \tau \nu$	0.62 ± 0.05		0.47-0.55	$0.33^{+0.14}_{-0.11}$			
$B_s \rightarrow D_s^* e \nu$	5.3 ± 0.5	2.5 ± 0.1	5.1-5.8		5.2 ± 0.6	7.49-7.66	1.89-6.61
$B_s \rightarrow D_s^* \tau \nu$	1.3 ± 0.1		1.2-1.3		$1.3^{+0.2}_{-0.1}$		

Table 3: Comparison of theoretical predictions for the branching fractions of semileptonic decays $B_s \rightarrow D_s^{(*)} l \nu$ (in %).

$D_s(2S)$ and vector $D_s^*(2S)$ mesons have close values.

Our predictions for the branching fractions of the semileptonic B_s decays to orbitally excited D_s mesons are given in Table 5 in comparison with other calculations. We find that decays to D_{s1} and D_{s2}^* mesons are dominant. First we compare with our previous calculation [15] which was performed in the framework of the heavy quark expansion. We give results found in the infinitely heavy quark limit ($m_Q \rightarrow \infty$) and with the account of first order $1/m_Q$ corrections. It was argued [15] that $1/m_Q$ corrections are large and their inclusion significantly influences the decays rates. The large effect of subleading heavy quark corrections was found to be a consequence of the vanishing of the leading order contributions to the decay matrix elements, due to heavy quark spin-flavour symmetry, at the point of zero recoil of the final charmed meson, while the subleading order contributions do not vanish at this kinematical point. Here we calculated the decay rates without application of the heavy quark expansion. We find that nonperturbative results agree well with the ones obtained with the account of the leading order $1/m_Q$ corrections [15]. This means that the higher order in $1/m_Q$ corrections are small, as was expected. Then we compare our predictions with the results of calculations in other approaches. The authors of Refs. [16, 13] employ different types of constituent quark models for their calculations. Light cone and three point QCD sum rules are used in Refs. [11]. In general we find reasonable agreement between our predictions and results of Refs. [16, 11], but results of the quark model calculations [13] are slightly larger.

The first experimental measurement of the semileptonic decay $B_s \rightarrow D_{s1} \mu \nu$ was done by the D0 Collaboration [17]. The branching fraction was obtained by assuming that the D_{s1} production in semileptonic decay comes entirely from the B_s decay and using a prediction for $Br(D_{s1} \rightarrow D^* K_S^0) = 0.25$. Its value $Br(B_s \rightarrow D_{s1} X \mu \nu)_{D0} = (1.03 \pm 0.20 \pm 0.17 \pm 0.14)\%$ is in good agreement with our prediction 0.84 ± 0.9 given in Table 5.

Recently the LHCb Collaboration [18] reported the first observation of the orbitally excited D_{s2}^* meson in the semileptonic B_s decays. The decay to the D_{s1} meson was also observed. The measured branching fractions relative to the total B_s semileptonic rate are $Br(B_s \rightarrow D_{s2}^* X \mu \nu)/Br(B_s \rightarrow X \mu \nu)_{LHCb} = (3.3 \pm 1.0 \pm 0.4)\%$, $Br(B_s \rightarrow D_{s1} X \mu \nu)/Br(B_s \rightarrow X \mu \nu)_{LHCb} = (5.4 \pm 1.2 \pm 0.5)\%$. The D_{s2}^*/D_{s1} event ratio is found to be $Br(B_s \rightarrow D_{s2}^* X \mu \nu)/Br(B_s \rightarrow D_{s1} X \mu \nu)_{LHCb} = 0.61 \pm 0.14 \pm 0.05$. These values can be compared with our predictions if we assume that decays to D_{s1} and D_{s2}^* mesons give dominant contributions to the ratios. Summing up the semileptonic B_s decay branching fractions to ground state, first radial and orbital excitations of D_s mesons we get for the total B_s semileptonic rate $Br(B_s \rightarrow X \mu \nu) =$

Decay	Br
$B_s \rightarrow D_s(2S) e \nu$	0.27 ± 0.03
$B_s \rightarrow D_s(2S) \tau \nu$	0.011 ± 0.001
$B_s \rightarrow D_s^*(2S) e \nu$	0.38 ± 0.04
$B_s \rightarrow D_s^*(2S) \tau \nu$	0.015 ± 0.002

Table 4: Predictions for the branching fractions of semileptonic decays $B_s \rightarrow D_s^{(*)}(2S) l \nu$ (in %).

Decay	this paper	$m \rightarrow \infty$ [15]	with $1/m_Q$ [15]	[16]	[13]	[11]
$B_s \rightarrow D_{s0}^* e \nu$	0.36 ± 0.04	0.10	0.37	0.443	0.49-0.571	$0.23^{+0.12}_{-0.10}$
$B_s \rightarrow D_{s0}^* \tau \nu$	0.019 ± 0.002					$0.057^{+0.028}_{-0.023}$
$B_s \rightarrow D_{s1}' e \nu$	0.19 ± 0.02	0.13	0.18	0.174-0.570	0.752-0.869	
$B_s \rightarrow D_{s1}' \tau \nu$	0.015 ± 0.002					
$B_s \rightarrow D_{s1} e \nu$	0.84 ± 0.09	0.36	1.06	0.477		
$B_s \rightarrow D_{s1} \tau \nu$	0.049 ± 0.005					
$B_s \rightarrow D_{s2}^* e \nu$	0.67 ± 0.07	0.56	0.75	0.376		
$B_s \rightarrow D_{s2}^* \tau \nu$	0.029 ± 0.003					

Table 5: Comparison of the predictions for the branching fractions of the semileptonic decays $B_s \rightarrow D_{sJ}^{(*)} l \nu$ (in %).

	$B_s \rightarrow K$			$B_s \rightarrow K^*$						
	f_+	f_0	f_T	V	A_0	A_1	A_2	T_1	T_2	T_3
$F(0)$	0.284	0.284	0.236	0.291	0.289	0.287	0.286	0.238	0.238	0.122
$F(q_{\max}^2)$	5.42	0.459	0.993	3.06	2.10	0.581	0.953	1.28	0.570	0.362
σ_1	-0.370	-0.072	-0.442	-0.516	-0.383	0	1.05	-1.20	0.241	0.521
σ_2	-1.41	-0.651	0.082	-2.10	-1.58	-1.06	0.074	-2.44	-0.857	-0.613

Table 6: Calculated form factors of weak $B_s \rightarrow K^{(*)}$ transitions.

$(10.2 \pm 1.0)\%$. Then using the calculated values from Table 5 we get $Br(B_s \rightarrow D_{s2}^* \mu \nu)/Br(B_s \rightarrow X \mu \nu)_{\text{theor}} = (6.5 \pm 1.2)\%$, $Br(B_s \rightarrow D_{s1} \mu \nu)/Br(B_s \rightarrow X \mu \nu)_{\text{theor}} = (8.2 \pm 1.6)\%$, and $Br(B_s \rightarrow D_{s2}^* \mu \nu)/Br(B_s \rightarrow D_{s1} \mu \nu)_{\text{theor}} = 0.79 \pm 0.14$. The predicted central values are larger than experimental ones, but the results agree with experiment within 2σ .

The following total semileptonic B_s branching ratios were found: (1) for decays to ground state $D_s^{(*)}$ mesons $Br(B_s \rightarrow D_s^{(*)} e \nu) = (7.4 \pm 0.7)\%$ and $Br(B_s \rightarrow D_s^{(*)} \tau \nu) = (1.92 \pm 0.15)\%$; (2) for decays to radially excited $D_s^{(*)}(2S)$ mesons $Br(B_s \rightarrow D_s^{(*)}(2S) e \nu) = (0.65 \pm 0.06)\%$ and $Br(B_s \rightarrow D_s^{(*)}(2S) \tau \nu) = (0.026 \pm 0.003)\%$; (3) for decays to orbitally excited $D_{sJ}^{(*)}$ mesons $Br(B_s \rightarrow D_{sJ}^{(*)} e \nu) = (2.1 \pm 0.2)\%$ and $Br(B_s \rightarrow D_{sJ}^{(*)} \tau \nu) = (0.11 \pm 0.01)\%$. We see that these branching fractions significantly decrease with excitation. Therefore, we can conclude that considered decays give the dominant contribution to the total semileptonic branching fraction $Br(B_s \rightarrow D_s e \nu + \text{anything})$. Summing up these contributions we get the value $(10.2 \pm 1.0)\%$, which agrees with the experimental value $Br(B_s \rightarrow D_s e \nu + \text{anything})_{\text{Exp.}} = (7.9 \pm 2.4)\%$ [6].

4 Charmless semileptonic B_s decays

Comparing the invariant form factor decomposition (4)–(6) with the results of the calculations of the weak current matrix element in our model we determine the form factors in the whole accessible kinematical range through the overlap integrals of the meson wave functions. The explicit expressions are given in Ref. [4]. For the numerical evaluations of the corresponding overlap integrals we use the quasipotential wave functions of B_s and $K^{(*)}$ mesons obtained in their mass spectra calculations [7]. The weak $B_s \rightarrow K^{(*)}$ transition form factors can be

approximated with good accuracy by Eqs. (7), (8). The obtained values $F(0)$ and $\sigma_{1,2}$ are given in Table 6.

Using these form factors we get predictions for the total decay rates. The kinematical range accessible in the heavy-to-light $B_s \rightarrow K^{(*)}$ transitions is very broad, making knowledge of the q^2 dependence of the form factors to be an important issue. Therefore, the explicit determination of the momentum dependence of the weak decay form factors in the whole q^2 range without any additional assumptions is an important advantage of our model.

The calculated branching fractions of the semileptonic $B_s \rightarrow K^{(*)}l\nu_l$ decays are presented in Table 7 in comparison with other theoretical predictions [19, 20]. The perturbative QCD factorization approach is used in Ref. [19], while in Ref. [20] light cone sum rules are employed. From the comparison in Table 7 we see that all theoretical predictions for the B_s semileptonic branching fractions agree within uncertainties. This is not surprising since these significantly different approaches predict close values of the corresponding weak form factors.

We employ the same approach for the calculation of the form factors of the weak B_s decays to orbitally excited $K_J^{(*)}$ mesons. The total semileptonic $B_s \rightarrow K_J^{(*)}l\nu_l$ branching fractions are given in Table 8. We see that our model predicts close values (about 1×10^{-4}) for all semileptonic B_s branching fractions to the first orbitally excited $K_J^{(*)}$ mesons. Indeed, the difference between branching fractions is less than a factor of 2. This result is in contradiction to the dominance of specific modes (by more than a factor of 4) in the heavy-to-heavy semileptonic $B \rightarrow D_J^{(*)}l\nu_l$ and $B_s \rightarrow D_{sJ}^{(*)}l\nu_l$ decays, but it is consistent with predictions for the corresponding heavy-to-light semileptonic B decays to orbitally excited light mesons [21]. The above mentioned suppression of some heavy-to-heavy decay channels to orbitally excited heavy mesons was mostly pronounced in the heavy quark limit and then slightly reduced by the heavy quark mass corrections which are found to be large. Thus our result once again indicates that the s quark cannot be treated as a heavy one and should be considered to be light instead, as we always did in our calculations.

In Table 8 we compare our predictions for the semileptonic B_s branching fractions to orbitally excited $K_J^{(*)}$ mesons with previous calculations [22, 23, 24, 25, 11, 26]. The consideration in Ref. [22] is based on QCD sum rules. The light cone sum rules are used in Refs. [23, 25], while Refs. [24, 11, 26] employ the perturbative QCD approach. Reasonable agreement between our results and other predictions [22, 23, 26] is observed for the semileptonic B_s decays to the scalar and tensor K mesons. The values of Ref. [24] are almost a factor 3 higher. For the semileptonic B_s decays to axial vector K mesons predictions are significantly different even within rather large errors. Therefore experimental measurement of these decay branching fractions can help to discriminate between theoretical approaches.

We see that total branching fractions of semileptonic B_s decays to ground and first orbitally excited K mesons have close values of about 5×10^{-4} . Summing up these contributions, we get $(9.5 \pm 1.0) \times 10^{-4}$. This value is almost 2 orders of magnitude lower than our prediction for the corresponding sum of branching fractions of the semileptonic B_s to D_s mesons as it was expected from the ratio of CKM matrix elements $|V_{ub}|$ and $|V_{cb}|$. Therefore the total semileptonic B_s

Decay	this paper	[19]	[20]
$B_s \rightarrow K e \nu_e$	1.64 ± 0.17	$1.27^{+0.49}_{-0.30}$	1.47 ± 0.15
$B_s \rightarrow K \tau \nu_\tau$	0.96 ± 0.10	$0.778^{+0.268}_{-0.201}$	1.02 ± 0.11
$B_s \rightarrow K^* e \nu_e$	3.47 ± 0.35		2.91 ± 0.26
$B_s \rightarrow K^* \tau \nu_\tau$	1.67 ± 0.17		1.58 ± 0.13

Table 7: Comparison of theoretical predictions for the branching fractions of semileptonic decays $B_s \rightarrow K^{(*)}l\nu_l$ (in 10^{-4}).

Decay	this paper	[22]	[23]	[24]	[25]	[11]	[26]
$B_s \rightarrow K_0^* e \nu_e$	0.71 ± 0.14	$0.36^{+0.38}_{-0.24}$	$1.3^{+1.3}_{-0.4}$	$2.45^{+1.77}_{-1.05}$			
$B_s \rightarrow K_0^* \tau \nu_\tau$	0.21 ± 0.04		$0.52^{+0.57}_{-0.18}$	$1.09^{+0.82}_{-0.47}$			
$B_s \rightarrow K_1(1270) e \nu_e$	1.41 ± 0.28				$4.53^{+1.67}_{-2.05}$	$5.75^{+3.49}_{-2.89}$	
$B_s \rightarrow K_1(1270) \tau \nu_\tau$	0.30 ± 0.06					$2.62^{+1.58}_{-1.31}$	
$B_s \rightarrow K_1(1400) e \nu_e$	0.97 ± 0.20				$3.86^{+1.43}_{-1.75}$	$0.03^{+0.05}_{-0.02}$	
$B_s \rightarrow K_1(1400) \tau \nu_\tau$	0.25 ± 0.05					$0.01^{+0.02}_{-0.01}$	
$B_s \rightarrow K_2^* e \nu_e$	1.33 ± 0.27						$0.73^{+0.48}_{-0.33}$
$B_s \rightarrow K_2^* \tau \nu_\tau$	0.36 ± 0.07						$0.25^{+0.17}_{-0.12}$

Table 8: Comparison of theoretical predictions for the branching fractions of semileptonic decays $B_s \rightarrow K_J^{(*)} l \nu_l$ (in 10^{-4}).

	$B_s \rightarrow \eta_s$			$B_s \rightarrow \varphi$						
	f_+	f_0	f_T	V	A_0	A_1	A_2	T_1	T_2	T_3
$F(0)$	0.384	0.384	0.301	0.406	0.322	0.320	0.318	0.275	0.275	0.133
$F(q_{\text{max}}^2)$	3.31	0.604	1.18	2.74	1.64	0.652	0.980	1.47	0.675	0.362
σ_1	-0.347	-0.120	-0.897	-0.861	-0.104	0.133	1.11	-0.491	0.396	0.639
σ_2	-1.55	-0.849	-1.34	-2.74	-1.19	-1.02	0.105	-1.90	-0.811	-0.531

Table 9: Calculated form factors of weak $B_s \rightarrow \eta_s$ and $B_s \rightarrow \varphi$ transitions.

decay branching fraction is dominated by the decays to D_s mesons and in our model is equal to $(10.3 \pm 1.0)\%$ in agreement with the experimental value $Br(B_s \rightarrow X e \nu_e)_{\text{Exp.}} = (9.5 \pm 2.7)\%$ [6].

5 Rare semileptonic B_s decays

Now we apply our model for the consideration of the rare B_s decays. Using described above method we explicitly determine the form factors in the whole accessible kinematical range through the overlap integrals of the meson wave functions. They again can be approximated with good accuracy by Eqs. (7), (8). The obtained values of $F(0)$ and $\sigma_{1,2}$ are given in Table 9. Using these form factors we consider the rare semileptonic decays. In the calculations the usual factorization of short-distance (described by Wilson coefficients) and long-distance (which matrix elements are proportional to hadronic form factors) contributions in the effective Hamiltonian for the $b \rightarrow s$ transitions is employed. The effective Wilson coefficient c_9^{eff} contains additional perturbative and long-distance contributions. The long-distance (nonperturbative) contributions are assumed to originate from the $c\bar{c}$ vector resonances (J/ψ , $\psi(2S)$, $\psi(3770)$, $\psi(4040)$, $\psi(4160)$ and $\psi(4415)$) and have a usual Breit-Wigner structure. In Fig. 2 we confront our predictions for differential branching fractions, dBr/dq^2 , and the longitudinal polarization fraction, F_L , with experimental data from PDG (CDF) [6] and recent LHCb [27] data. By solid lines we show results for the nonresonant branching fractions, where long-distance contributions of the charmonium resonances to the coefficient c_9^{eff} are neglected. Plots given by the dashed lines contain such resonant contributions. For decays with the muon pair two largest peaks correspond to the contributions coming from the lowest vector charmonium states J/ψ and $\psi(2S)$, since they are narrow. The region of these resonance peaks is excluded in exper-

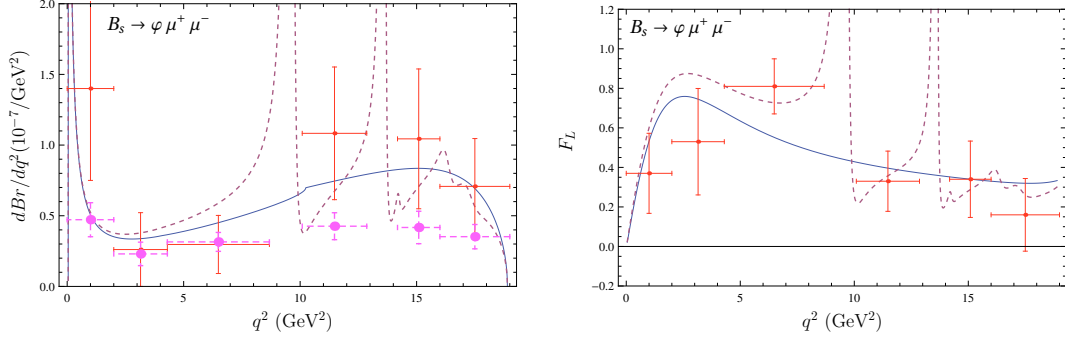


Figure 2: Comparison of theoretical predictions for the differential branching fractions $dBr(B_s \rightarrow \varphi \mu^+ \mu^-)/dq^2$ and the φ longitudinal polarization F_L with available experimental data.

imental studies of these decays. Contributions in the low recoil region originating from the higher vector charmonium states, which are above the open charm threshold, are significantly less pronounced. The LHCb values for the differential branching fractions in most q^2 bins are lower than the CDF ones, but experimental error bars are rather large. Our predictions lie just in between these experimental measurements. For the φ longitudinal polarization fraction, F_L , only LHCb data are available which agree with our results within uncertainties. the differential branching fractions, forward-backward asymmetry and longitudinal polarization fraction.

In Table 10 we present our predictions for the nonresonant branching fractions of the rare semileptonic B_s decays and compare them with previous calculations [28, 29, 30, 31, 20] and available experimental data [6, 27]. In Ref. [28] the form factors were calculated on the basis of the light-cone QCD sum rules within the soft collinear effective theory. The authors of Ref. [29] employ the light front and constituent quark models for the evaluation of the rare decay branching fractions. Three-point QCD sum rules are used for the analysis of the rare semileptonic B_s decays into $\eta(\eta')$ and lepton pair in Ref. [30]. In Ref. [31] calculations are based on the light-front quark model, while light-cone sum rules in the framework of heavy quark effective field theory are applied in Ref. [20]. The analysis of the predictions given in Table 10 indicate that these significantly different approaches give close values of order 10^{-7} for the rare semileptonic $B_s \rightarrow \varphi(\eta') l^+ l^-$ decay branching fractions and of order 10^{-8} for $B_s \rightarrow K^{(*)} l^+ l^-$ decays. Experimental data are available for the branching fraction of the $B_s \rightarrow \varphi \mu^+ \mu^-$ decay only. As we see from the table all theoretical predictions are well consistent with each other and experimental data for the $B_s \rightarrow \varphi \mu^+ \mu^-$ decay from PDG [6]. Note that very recently the LHCb Collaboration [27] also reported measurement of this decay branching fraction with the value $7.07^{+0.97}_{-0.94} \times 10^{-7}$ which is somewhat lower than previous measurements. Our prediction is consistent with the latter value within 2σ .

6 Conclusions

The form factors parametrizing the transition matrix of the weak current between the B_s and heavy (D_s^* , $D_{sJ}^{(*)}$) or light ($K^{(*)}$, $K_J^{(*)}$, $\eta(\varphi)$) mesons were calculated on the basis of the relativistic quark model with the QCD-motivated quark-antiquark interaction potential. All

Decay	this paper	[28]	[29]	[30]	[31]	[20]	Exp.[6]
$B_s \rightarrow \eta \mu^+ \mu^-$	3.8 ± 0.4	3.4 ± 1.8	3.12	2.30 ± 0.97	2.4	1.2 ± 0.12	
$B_s \rightarrow \eta \tau^+ \tau^-$	0.90 ± 0.09	1.0 ± 0.55	0.67	0.373 ± 0.156	0.58	0.34 ± 0.04	
$B_s \rightarrow \eta \nu \bar{\nu}$	23.1 ± 2.3	29 ± 15	21.7	13.5 ± 5.6	17		
$B_s \rightarrow \eta' \mu^+ \mu^-$	3.2 ± 0.3	2.8 ± 1.5	3.42	2.24 ± 0.94	1.8		
$B_s \rightarrow \eta' \tau^+ \tau^-$	0.39 ± 0.04	0.47 ± 0.25	0.43	0.280 ± 0.118	0.26		
$B_s \rightarrow \eta' \nu \bar{\nu}$	19.7 ± 2.0	24 ± 13	23.8	13.3 ± 5.5	13		
$B_s \rightarrow \varphi \mu^+ \mu^-$	11.6 ± 1.2		16.4			11.8 ± 1.1	$12.3^{+4.0}_{-3.4}$
$B_s \rightarrow \varphi \tau^+ \tau^-$	1.5 ± 0.2		1.51			1.23 ± 0.11	
$B_s \rightarrow \varphi \nu \bar{\nu}$	79.6 ± 8.0		116.5				< 54000
$B_s \rightarrow K \mu^+ \mu^-$	0.24 ± 0.03				0.14	0.199 ± 0.021	
$B_s \rightarrow K \tau^+ \tau^-$	0.059 ± 0.006				0.03	0.074 ± 0.007	
$B_s \rightarrow K \nu \bar{\nu}$	1.42 ± 0.14				1.01		
$B_s \rightarrow K^* \mu^+ \mu^-$	0.44 ± 0.05					0.38 ± 0.03	
$B_s \rightarrow K^* \tau^+ \tau^-$	0.075 ± 0.008					0.050 ± 0.004	
$B_s \rightarrow K^* \nu \bar{\nu}$	3.0 ± 0.3						

Table 10: Comparison of theoretical predictions for the nonresonant branching fractions of the rare semileptonic B_s decays and available experimental data (in 10^{-7}).

relativistic effects, including boosts of the meson wave functions and contributions of the intermediate negative-energy states, were consistently taken into account. The main advantage of the adopted approach consists in that it allows the determination of the momentum transfer dependence of the form factors in the whole accessible kinematical range. Therefore no additional assumptions and ad hoc extrapolations are needed for the description of the weak decay processes which have rather broad kinematical range. This significantly improves the reliability of the obtained results.

The calculated form factors were used for considering the semileptonic and rare B_s decays. The differential and total decay branching fractions as well as asymmetry and polarization parameters were evaluated. The obtained results were confronted with previous investigations based on significantly different theoretical approaches and available experimental data. Good agreement of our predictions with measured values is observed.

The authors are grateful to A. Ali, D. Ebert, C. Hambrock, M. A. Ivanov, V. A. Matveev, A. Sibidanov and V. I. Savrin for useful discussions. This work was supported in part by the Russian Foundation for Basic Research under Grant No.12-02-00053-a.

References

- [1] R. Louvot *et al.* [Belle Collaboration], Phys. Rev. Lett. **102**, 021801 (2009).
- [2] R. Aaij *et al.* [LHCb Collaboration], Phys. Lett. B **698**, 115 (2011); Phys. Lett. B **709**, 50 (2012).
- [3] H. Ha *et al.* [Belle Collaboration], Phys. Rev. D **83**, 071101 (2011); J. P. Lees *et al.* [BaBar Collaboration], Phys. Rev. D **86**, 092004 (2012); A. Sibidanov *et al.* [Belle Collaboration], Phys. Rev. D **88**, 032005 (2013).
- [4] R. N. Faustov and V. O. Galkin, Phys. Rev. D **87**, 034033 (2013); Phys. Rev. D **87**, 094028 (2013); Eur. Phys. J. C **73**, 2593 (2013).
- [5] D. Ebert, R. N. Faustov and V. O. Galkin, Phys. Rev. D **75**, 074008 (2007).
- [6] J. Beringer *et al.* [Particle Data Group], Phys. Rev. D **86**, 010001 (2012).

- [7] D. Ebert, R. N. Faustov and V. O. Galkin, Phys. Rev. D **67**, 014027 (2003); Phys. Rev. D **79**, 114029 (2009); Eur. Phys. J. C **71**, 1825 (2011).
- [8] G. Kramer and W. F. Palmer, Phys. Rev. D **46**, 3197 (1992).
- [9] P. Blasi, P. Colangelo, G. Nardulli and N. Paver, Phys. Rev. D **49**, 238 (1994).
- [10] X. J. Chen, H. F. Fu, C. S. Kim and G. L. Wang, J. Phys. G **39**, 045002 (2012).
- [11] R. -H. Li, C. -D. Lu and Y. -M. Wang, Phys. Rev. D **80**, 014005 (2009).
- [12] G. Li, F. -I. Shao and W. Wang, Phys. Rev. D **82**, 094031 (2010).
- [13] S. -M. Zhao, X. Liu and S. -J. Li, Eur. Phys. J. C **51**, 601 (2007).
- [14] K. Azizi and M. Bayar, Phys. Rev. D **78**, 054011 (2008); K. Azizi, Nucl. Phys. B **801**, 70 (2008).
- [15] D. Ebert, R. N. Faustov and V. O. Galkin, Phys. Rev. D **61**, 014016 (2000).
- [16] J. Segovia *et al.* Phys. Rev. D **84**, 094029 (2011).
- [17] V. M. Abazov *et al.* [D0 Collaboration], Phys. Rev. Lett. **102**, 051801 (2009).
- [18] R. Aaij *et al.* [LHCb Collaboration], Phys. Lett. B **698**, 14 (2011); P. Urquijo, arXiv:1102.1160 [hep-ex].
- [19] W. -F. Wang and Z. -J. Xiao, Phys. Rev. D **86**, 114025 (2012).
- [20] Y. -L. Wu, M. Zhong and Y. -B. Zuo, Int. J. Mod. Phys. A **21**, 6125 (2006).
- [21] D. Ebert, R. N. Faustov and V. O. Galkin, Phys. Rev. D **85**, 054006 (2012).
- [22] M. -Z. Yang, Phys. Rev. D **73**, 034027 (2006) [Erratum-ibid. D **73**, 079901 (2006)].
- [23] Y. -M. Wang, M. J. Aslam and C. -D. Lu, Phys. Rev. D **78**, 014006 (2008).
- [24] R. -H. Li, C. -D. Lu, W. Wang and X. -X. Wang, Phys. Rev. D **79**, 014013 (2009).
- [25] K. -C. Yang, Phys. Rev. D **78**, 034018 (2008).
- [26] W. Wang, Phys. Rev. D **83**, 014008 (2011).
- [27] R. Aaij *et al.* [LHCb Collaboration], JHEP **1307**, 084 (2013).
- [28] M. V. Carlucci, P. Colangelo and F. De Fazio, Phys. Rev. D **80**, 055023 (2009).
- [29] C. Q. Geng and C. C. Liu, J. Phys. G **29**, 1103 (2003).
- [30] K. Azizi, R. Khosravi and F. Falahati, Phys. Rev. D **82**, 116001 (2010).
- [31] H. -M. Choi, J. Phys. **37**, 085005 (2010).